Rationally designed nanostructures for surface-enhanced Raman spectroscopy

Matthew J. Banholzer, Jill E. Millstone, Lidong Qin and Chad A. Mirkin*

Received 23rd January 2008
First published as an Advance Article on the web 26th March 2008
DOI: 10.1039/b710915f

Research on surface-enhanced Raman spectroscopy (SERS) is an area of intense interest because the technique allows one to probe small collections of, and in certain cases, individual molecules using relatively straightforward spectroscopic techniques and nanostructured substrates. Researchers in this area have attempted to develop many new technological innovations including high sensitivity chemical and biological detection systems, labeling schemes for authentication and tracking purposes, and dual scanning-probe/spectroscopic techniques that simultaneously provide topographical and spectroscopic information about an underlying surface or nanostructure. However, progress has been hampered by the inability of researchers to fabricate substrates with the high sensitivity, tunability, robustness, and reproducibility necessary for truly practical and successful SERS-based systems. These limitations have been due in part to a relative lack of control over the nanoscale features of Raman substrates that are responsible for the enhancement. With the advent of nanotechnology, new approaches are being developed to overcome these issues and produce substrates with higher sensitivity, stability, and reproducibility. This *tutorial review* focuses on recent progress in the design and fabrication of substrates for surface-enhanced Raman spectroscopy, with an emphasis on the influence of nanotechnology.

Introduction

Nanostructured materials often exhibit properties that are radically different from bulk materials of the same composition.[1] Nowhere is this effect more apparent than in the interactions of light with matter. Investigations in the burgeoning field of nanophotonics have demonstrated that certain nanostructures exhibit previously unanticipated behaviors. Dielectric materials have been arranged on the 100 nm length scale to halt light and steer it in new directions, and semiconductor nanocrystals have been used to produce highly fluorescent and photostable probes with emission wavelengths that correlate with particle size.[1] The collective oscillation of surface electrons on nanostructured conducting materials has been leveraged for numerous purposes, one of the most important being the amplification of optical processes such as Raman scattering. Indeed, the discovery of surface-enhanced Raman spectroscopy (SERS) was made approximately 30 years ago, and this phenomenon catalyzed a worldwide effort to explore its origins, maximize it, and harness its potential in fields ranging from plasmonics to diagnostics.

The phenomenon of SERS is generally explained by a combination of an electromagnetic (EM) mechanism describing the surface electron movement in the substrate and a chemical mechanism related to charge transfer (CT) between the substrate and the analyte molecules.[2,3] For the chemical

Department of Chemistry and International Institute for Nanotechnology, Northwestern University, 2145 Sheridan Road, Evanston, IL 60208-3113, USA. E-mail: chadnano@northwestern.edu; Fax: 847-467-5123; Tel: 847-467-7302

Matthew J. Banholzer was born in Niskayuna, NY and grew up in various cities in New York and Ohio. In 2006 he earned a B.A. in Chemistry from Cornell University where he worked on nanoparticle ligand design with Profs. Francis DiSalvo and Ulrich Wiesner. He is currently working towards a Ph.D. in Materials Chemistry under the supervision of Chad A. Mirkin at Northwestern University on plasmonics.

Jill E. Millstone was born in Detroit, MI and raised in Jacksonville, FL. In 2003, she earned her B.S. in both Chemistry and English from Carnegie Mellon University, where she also studied conducting polymers in the laboratory of Prof. Richard McCullough. She is currently a Ph.D. candidate in Materials Chemistry at Northwestern University working under the direction of Chad A. Mirkin.

Lidong Qin was born and grew up in Lu'an city, Anhui Province of China. He received his B.S. degree (1999) in Chemistry and M.S. in Polymer Chemistry and Physics (2002) from Jilin University, China. He completed his Ph.D. in Chemistry at Northwestern University under the supervision of Chad A. Mirkin in 2007 and is now working as a postdoctoral researcher at California Institute of Technology.

Chad A. Mirkin is the Director of the Northwestern International Institute for Nanotechnology, the Rathmann Prof. of Chemistry, Prof. of Medicine and Prof. of Materials Science & Engineering. He has authored over 320 manuscripts and 70 issued patents, founded the companies Nanosphere and NanoInk, and co-founded the journal Small. He has received over 50 national and international chemistry awards.

enhancement process, it is thought that the metal aids in CT excitations between the highest occupied molecular orbital (HOMO) and the lowest unoccupied molecular orbital (LUMO) of the adsorbate. These excitations are possible if the Fermi level of the metal is approximately halfway between the HOMO and LUMO of the adsorbate, which in turn allows CT processes to occur at approximately half the energy of the inherent intramolecular excitations. Naturally, this effect varies from molecule to molecule, but because the energetically lowest-lying CT process is in the near ultraviolet for most organic molecules, this metal-aided process occurs in the visible spectrum.

Of the two dominant processes, the EM mechanism usually provides the larger contribution to enhancement and, unlike the CT mechanism, its effects are uniform across all molecule types. It is principally this process that is tuned and manipulated by modifying the properties of a substrate designed for SERS.[3] The EM enhancement of SERS is often mediated by the surface plasmon resonance (SPR) of the substrate. The SPR of a metal can be observed when, upon illumination with light, a nanostructure (random or ordered) sustains collective oscillations of its surface electrons; it is this ensemble movement that is termed a SPR. When the excitation light is resonant with a plasmon, the metal particle will emit EM radiation coherent with the exciting field. The radiation generated by this process greatly increases the local field experienced by a molecule near the plasmonic structure (where ''near'' is the length scale of near-field radiation; for this application typically less than 20 nm). After a few femtoseconds, a steady state is established in which a distribution of electric field intensities ($|E|$) is created and large increases in intensities are possible at regions near the metal nanostructure. The nanostructure not only enhances the incident laser field (enhancing the intensity of radiation the Raman active molecule encounters, leading to more total photon–molecule interactions) but also the Raman scattered field (enhancing the intensity of the Raman scattered light, leading to more detectable scattered photons); since it has been established that the Raman scattering enhancement scales roughly as $|E|^4$, extremely large SERS enhancements ($>10^8$ when combined with the CT mechanism) are possible with only modest EM field augmentations.

Nanostructured surfaces often lead to SPR formation; by varying the nanostructure (*e.g.* pitch, periodicity, size), different plasmon frequencies and modes can be harnessed for use in a given application. To generate these surfaces, researchers initially relied on either randomly roughened electrodes or colloidal aggregates composed of randomly dispersed particles. Baker and Moore have written an excellent review that summarizes progress in this area of research.[4] Work focusing on the mechanism and optimization of the SERS effect has laid the foundation for applications that take advantage of the extraordinary sensitivity afforded by the technique.

While experiments with randomly roughened surfaces have generated a great deal of interesting and essential data relevant to SERS, there is inherent irreproducibility associated with such strategies since minor changes in surface morphology can lead to dramatic changes in enhancement. Thus, in recent years, many techniques have been developed to generate SERS substrates that have deliberately designed, periodic surface structures. Surfaces with these defined architectures then allow both elementary and technological studies that bring SERS closer to being a reliable spectroscopic tool and a basis for future applications. In this regard, attempts to make SERS-optimized nanostructures and nanostructured surfaces have been made by a wide variety of techniques, including nanosphere lithography[5–8] and related colloidal particle and nanowire techniques, on-wire lithography,[9,10] e-beam lithography,[11,12] and nanoimprint lithography.[13]

In evaluating SERS activity, many of these authors report the ''enhancement factor'' (EF) of their nanostructured substrate, which is a measure of the ability of the substrate to enhance the weak Raman signal from analyte molecules. There are many possible rigorous definitions of this value, and the reader is urged to carefully consider the methodology of each paper. A study by Etchegoin and co-workers discusses this issue in depth.[14] Further complications arise depending on confounding factors such as contributions from molecular resonance in certain analytes such as Rhodamine 6G (R6G) or Methylene Blue (MB). Thus, an effort has been made to note which analyte molecule each source used to allow the reader to better evaluate the experiments. Due to the complexity of this issue and the brevity of this review, EFs are included as reported by the original authors.

It is also worth noting that the nature of the surface modification is another important factor for SERS enhancement. The packing of multi- or mono-layers, as well as the strength and type of substrate–analyte interactions may affect SERS behavior. While beyond the scope of this review, this concept can be important when describing these systems, and the reader is advised to keep this issue also in mind while reading the following summaries.

This tutorial review describes recent ($\sim$5 years or less) progress in the rational design and engineering of SERS substrates that allow one to study the origins of enhancement, optimize the amplification factors, and replicate structures that provide consistent and optimized responses. In every case, the SERS activity of the substrate was demonstrated in the published work; interesting or promising substrates (such as SPR-harnessing ring/crescent shaped structures) without empirical verification of their SERS activity are not included in this review.

Most techniques developed in recent years can be divided into five different categories: large ensembles of nanoparticles used to structure a surface, isolated nanoparticle dimers (either in solution or on a surface), anisotropic nanoparticles and junctions formed between them, mechanical break or electromigrated metal gaps or junctions, and lithography techniques (Fig. 1). It should be noted that many engineered substrates could fit into a variety of different sections, but for the purposes of this review, efforts are made to group papers based on the emphasis of the original authors. Scanning probe-tip-enhanced methodologies[15–17] as well as the many bead—based methodologies for SERS[4,18] are beyond the scope of this review.

Nanoparticle-defined surfaces

The natural evolution of SERS substrates from roughened surfaces and colloids to rationally-designed nanomaterials

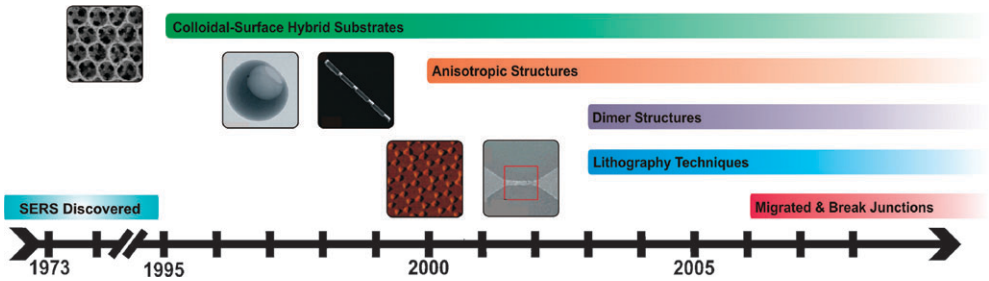

Fig. 1 Timeline of development of SERS substrates discussed in this paper. Insets are examples of each type of structure corresponding (from upper left to lower right) to refs. 22, 36, 9, 7, and 38.

combines the benefits of both of these progenitors into one elegant system. By positioning nanoparticles on a substrate, the SERS hotspots (areas of increased SERS activity) generated by colloidal junctions can be easily located and more readily controlled than if they were random colloidal aggregates. One of the earliest examples of this technique was demonstrated by Natan and co-workers, who made both Au and Ag nanoparticle (AuNP, AgNP) monolayers on inorganic, nonconductive coated substrates.[19] By functionalizing these substrates with a crosslinking molecule and dip-coating them with metal colloids, the authors observed Raman enhancement and low signal variation from substrate to substrate. For example, eight SiO_2 substrates functionalized with 12 nm diameter silver nanoparticles (AgNPs, crosslinked to the silica by 3-aminopropyltrimethoxysilane) exhibited 10% or less variation in integrated peak intensity from films using *trans*-1,2-bis(4-pyridyl)ethylene (BPE) as the analyte molecule. This approach was successful with a variety of SiO_x-coated substrates (*e.g.* quartz, plasma treated-Teflon, Formvar, ITO and Pt), with both Ag and Au nanoparticles. In addition, SERS response could be optimized by controlling factors such as immersion time during dip-coating, analyte solution concentration, and particle size. However, EFs were not reported.

The concept behind the work of Natan and co-workers was expanded and refined by Nie and co-workers, who developed nanostructured thin films by depositing monodisperse AgNPs on a polycarbonate membrane.[20] In this work, Nie and co-workers first fractionated AgNPs into different size groups ranging from 30 to over 100 nm. This preliminary purification procedure resulted in films with higher packing densities than most previous methods employed, which in turn allowed for more particle couplings and thus higher SERS enhancements. By rigorously controlling the particle size, density and number of layers, Nie and co-workers showed that the substrate optical properties such as excitation wavelength response could be tuned. The authors showed that by increasing the size of the AgNPs from approximately 90 to >100 nm can shift the most efficient excitation wavelength from 514 to 633 nm.

The above work was an important step in making more highly ordered nanoparticle-based substrates. However, the interparticle spacing, which is of paramount importance to EM enhancement mechanisms, could not be finely controlled. Halas and co-workers calculated this dependence and developed a system to more effectively harness incoming light using regularly spaced NPs. By building on theoretical work that modeled two nanoparticles as a pseudodimer, and drawing similarities to molecular orbital theory they argue that sub-10 nm gaps are optimal for SERS enhancement.[21] To prepare a substrate with the maximum possible amount of junctions with this optimized geometry, Halas *et al.* functionalized 50 nm AuNPs with cetyltrimethylammonium bromide (CTAB), redispersed the colloids in water and finally drop-cast the suspension onto indium-doped tin oxide (ITO) to create a monolayer of particles with an average interparticle distance of $\sim$8 nm. This gap provides the near-field enhancement needed to generate an appreciable SERS signal. Interestingly, the authors state that these NP arrays have complementary optoelectromagnetic properties to arrays generated by the nanosphere lithography approach (NSL, *vide infra*). The authors hypothesize that the self-assembled CTAB bilayer on the AuNPs generates a net positive charge on each particle which leads to electrostatic repulsion that prevents random aggregation. Finally, the authors claim an EF of 1×10^8 using *p*-mercaptoaniline (*p*MA) as the reporter, and that the substrates are stable for 30 days. However, these substrates degrade over longer times, only producing 50% of the initial SERS intensity after 90 days.

While immobilized colloids have proven interesting test beds for SERS, multiple groups have attempted to employ colloidal crystal (CC) techniques to generate structures with SERS functionalities. Because the templating particle size for all CC techniques can be varied, they allow tunability in the CC optical properties so that these substrates can be optimized for a given excitation wavelength. Among the first to demonstrate the feasibility of this approach were Velev and co-workers.[22] In their most recent work, Velev and co-workers used a "convective assembly" method to co-deposit large, 400–1000 nm latex particles and small, 10–20 nm AuNPs. Films were produced by dispensing a suspension of gold and latex particles between two glass slides: one that was horizontal and one held at an angle to the first, forming a "V" shape (Fig. 2(A) inset). By pulling the top slide along the bottom one with an electric motor, the meniscus of the suspension was dragged along the bottom plate and deposited a thin colloidal film. The deposited crystals were dried (during which the AuNPs settle into the voids in the larger latex particle array, pack into place, and form a solid matrix) and the latex spheres were dissolved with toluene. The thickness of the films could be controlled by modifying the concentration of the latex/Au NP suspension. The resulting Au films exhibited a 3D structure characteristic of the "inverse opal" morphology, which consists of a 3D network of thin lines duplicating the shape of

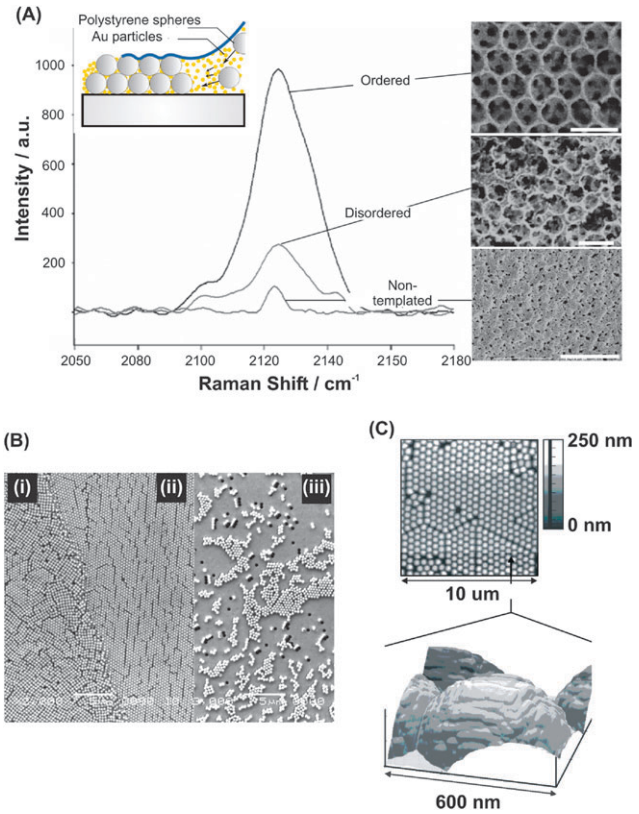

Fig. 2 Colloidal crystal techniques from refs. 5, 22 and 24. (A) (ref. 22) Effect of substrate structure on the SERS signal intensity. Characteristic sodium cyanide spectra and SEM images collected in the continuous sampling microfluidic flow cell for ordered latex-templated (top), disordered latex-templated (middle), and non-templated (bottom) SERS substrates. Scale bars are 1 mm (top and middle micrographs) and 10 mm (bottom micrograph). Inset is schematic of convective assembly technique. (B) (ref. 24) SEM images of three different regions of the nanostructured metallic substrate: (i) multilayer polystyrene nanoparticles, (ii) single-layer polystyrene nanoparticles, and (iii) randomly distributed self-assembled clusters and nanoholes. (C) (ref. 5) Ambient contact mode atomic force microscope image of 200 nm Ag over 542 nm diameter polystyrene spheres. (Top) Array of 10 μm × 10 μm spheres (bottom) 600 nm × 600 nm spheres of one sphere showing substructure roughness. (Reprinted with permission. Copyright 2002, 2005 and 2006, American Chemical Society and Elsevier Ltd.)

the interstitial regions of the larger close-packed latex spheres. Velev and co-workers used NaCN as their Raman reporter, and found that template substrates showed SERS intensities approximately one order of magnitude stronger than untemplated (but still rough) films. However, after heating to temperatures between 200 and 500 °C, a marked decrease in SERS activity occurs as the nanofeatures generated by the AuNPs degrade (Fig. 2(A)).

Techniques to generate structures with complementary morphology to those described above were employed by the groups of Fujishima,[23] Baia[24] and Van Duyne.[5] In these studies, the CC was used to generate opal, rather than inverse-opal, structured SERS substrates. These works used either 300 nm silica microspheres (MSs) assembled by vertical deposition (the substrate is raised in solution), 220 nm latex beads assembled by static solvent evaporation, or ~542 nm styrene spheres (assembly not stated), respectively. Fujishima and co-workers proceeded with metal functionalization by infiltrating the network with a mixture of 10 nm AgNPs and polymer. Upon calcination at 300 °C for 1 h in air, the copolymer is removed and an opal structure consisting of Ag-coated silica particles results. Baia *et al.* and Van Duyne *et al.*, on the other hand, evaporated metal directly over the opal structures, (a 54 nm thick Au film for the former group, 200 nm Ag for the latter), resulting in a pseudo-2D Au surface layer with opal morphology (Fig. 2(B), (C)).

Fujishima and co-workers found that their Ag-functionalized CC was 40 times more enhancing than a flat silver film, and three times more than from an electrochemically roughened substrate (*p*-toluenethiol was used to measure Raman response). The authors also noted that the recorded Raman signal was quite uniform in intensity (normalized standard deviation of 0.04 *vs.* 0.71 for randomly electrochemically roughened substrates), regardless of where the signal was collected.

Baia *et al.* note that different Au-coated CC packings (partial monolayer, full monolayer, multilayer) provide different EFs. In probing their R6G-functionalized system the highest signal amplifications were collected from substrate regions where regular single layers, randomly distributed clusters and nanocavities co-exist. Coated monolayers exhibited intermediate intensity and multilayer zones were reported to exhibit the least intensity. The authors justify this by stating that propagating plasmons responsible for the SERS effect over periodic structures are less efficient enhancers for local fields than local plasmons generated by junctions and gaps between nanospheres and inside of nanoholes.

Van Duyne and co-workers carried out electrochemical SERS work, running their SERS experiments in an electrochemical cell and testing the substrates' ability to generate large enhancement for both irreversibly (*e.g.* BPE) and reversibly (*e.g.* pyridine) bound analytes under a variety of applied potentials. The authors found that their substrates matched the SERS activity of electrodes prepared by oxidation–reduction cycling, however their substrates exhibited much greater stability *in situ* for measurements at a larger range of applied potentials.

Van Duyne and co-workers improved the use of evaporative films templated by micro or nanospheres by using atomic-later deposition to coat an Ag opaline structure with a sub-1 nm layer of aluminium oxide.[6] This procedure greatly increased the stability of the underlying Ag substrate; the alumina coated film can maintain its activity for over nine months which represents a seven-fold increase in temporal stability over previous methods. Interestingly, the enhancing properties of the substrate are not greatly affected by the alumina layer (the authors report SERS intensity decays by approximately one order of magnitude for every 2.8 nm of alumina). As an additional advantage, the alumina-modified substrates exhibit new types of surface chemistry, where the interaction between the analyte molecules and the surface allows for high adsorption of polar molecules (*e.g.* carboxylic acids). In this work, Van Duyne and co-workers were able to detect anthrax biomarkers (calcium dipicolinate, a *bacillus* spore byproduct) with a limit of detection of 1.9 μM.

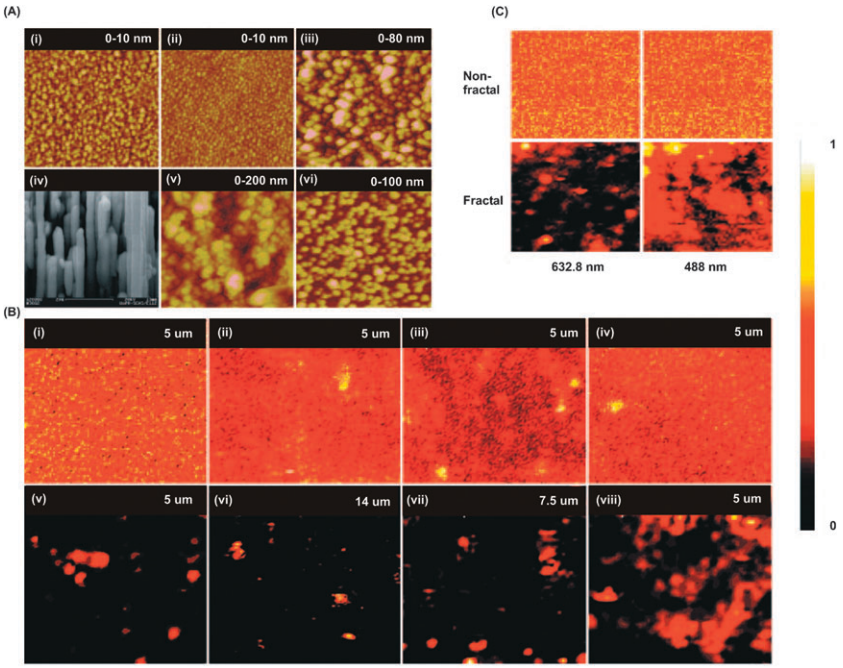

Fig. 3 Comparison of different Ag substrate types from ref. 25. (A) Topology of the various silver surfaces by AFM or scanning electron microscopy. (i) and (ii) Silver films 100 and 5 nm thick made by thermal evaporation. (iii) Compacted nanoparticle films. (iv) Nanorod arrays. (v) Cluster–cluster aggregated films. (vi) Mirror reaction films. The size of each image is 2 μm × 2 μm. The height scales are shown in the images. (B) Raman images of adsorbates (immersion oil or 4-mercaptopyridine). (i) 100- and (ii) 5-nm thick silver films by thermal evaporation. (iii) Silver nanoparticle films (called compacted nanoparticle films). (iv) Nanorod arrays. (v) Cluster–cluster aggregated films. (vi–viii) Mirror reaction films were formed by using the Tollens reaction. In (vi), the Tollens reaction time was 5 min, whereas in (vii) and (viii) the time was 2 min. All images were taken by scanning confocal Raman microscopy with excitation at 632.8 nm. The scan size is shown on the images. Note that each image is internally normalized to its maximum so that relative intensities between images cannot be compared. In particular, the hotspots on fractal surfaces have orders of magnitude more Raman scattering than counterparts of similar color on nonfractal surfaces. (C) Raman images of a single area on selected fractal and nonfractal surfaces for different excitation wavelengths. (upper) The Raman images of immersion oil on the 100-nm thick silver film. (lower) The Raman images of 4-mercaptopyridine adsorbed on cluster–cluster aggregated films. The size of each image is 5 μm × 5 μm. Note that each image is internally normalized to its maximum so that relative intensities between images cannot be compared. In particular, the hotspots on fractal surfaces have orders of magnitude more Raman scattering than counterparts of similar color on nonfractal surfaces. (Reprinted with permission. Copyright 2003, National Academy of Sciences, USA.)

All of the above work independently demonstrated how rationally designed substrates could increase SERS performance, but a comprehensive, internally controlled, investigation comparing different substrates was not attempted. To rigorously compare which nanostructures may be most interesting for SERS, Rothberg and co-workers carried out an empirical investigation of surface enhancement based on rational design across many structure types.[25] In their report, Rothberg and co-workers study continuous and discontinuous films formed by Ag evaporation, compacted nanoparticle films formed by covalent attachment of silver nanoparticles to a glass substrate, films of silver nanorods grown in aluminum oxide templates, cluster–cluster aggregated films formed by induced precipitation from suspensions of colloidal Ag particles, and films formed by the Tollens reaction for SERS response (Fig. 3(A)). The morphology of each substrate was primarily evaluated by AFM, and Raman enhancement was mapped and quantified *via* confocal Raman microscopy (Fig. 3(B)).

In their studies, fractal dimensionality, D, was calculated based on measurements of RMS roughness over the dimensions $L \times L$ *vs.* L, where L is length, and fitting the result to a power law from which D could be extracted. From this analysis, it was determined that substrates formed by deposited colloidal cluster–cluster aggregates and the Tollens reaction exhibited fractal character (the discovery that the Tollens reaction can produce fractal surfaces was novel in its own right). Coincidentally, these films exhibited the most dramatic SERS response, leading to the conclusion that fractal ($D \approx 1.5$) morphologies were most efficient at generating an electromagnetic field enhancement (not to be confused with an Raman enhancement factor), which the authors estimated was approximately 5×10^{13} (Fig. 3(C)). Regular, periodic, or smooth substrates had relatively little enhancement. For these fractal surfaces, Raman intensity distributions were reported to be extremely inhomogeneous and "hypersensitive" to the excitation polarization and wavelength, which could be a drawback to using such systems in a detection modality.

Citing previous literature results, Rothberg and co-workers proposed[25] that the plasmon normal modes responsible for Raman enhancement are concentrated in fractal aggregates because of the concentrated interaction between particle dipoles in the aggregate. Adsorbates near these hotspots are principally responsible for the large SERS signal. Since these hotspots occur at effectively random locations on the surface, this explains the observation of the random nature of Raman intensity distributions and polarization sensitivity. The authors conclude this

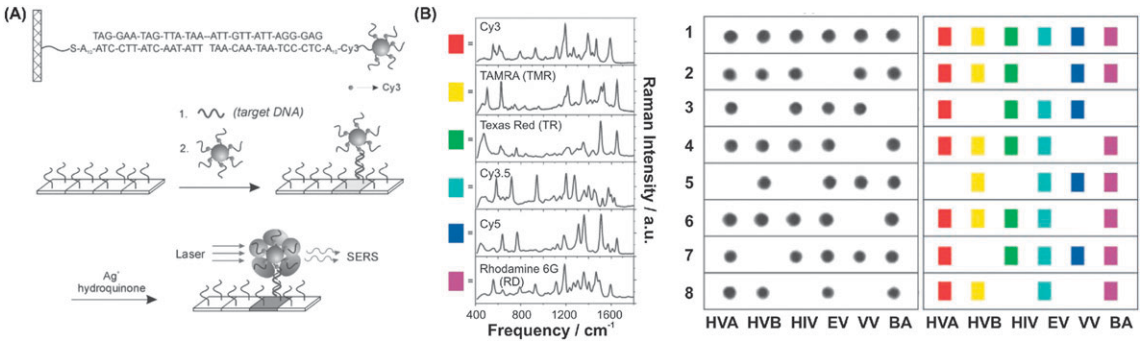

Fig. 4 Nanoparticle based detection assay from ref. 28. (A) Scheme of nanoparticle based detection assay. (B) (Left) The Raman spectra of six dye-labeled nanoparticle probes after Ag enhancing on a chip. Each dye correlates with a different color in a labeling scheme (see rectangular boxes). (Right) Flatbed scanner images of Ag-enhanced microarrays with the corresponding Raman spectra. The colored boxes correlate with the color-coded Raman spectra on left. (Reprinted with permission. Copyright 2002, AAAS.)

argument by noting that in the contrasting case of compact or periodic structures, the normal modes of the surface plasmons are instead delocalized over larger regions determined by long-range dipole–dipole interactions of the nanoparticle surface plasmons. However, it should be noted that fractal structure, while certainly beneficial in a SERS system, is not a prerequisite, and extremely large enhancements can be generated in the absence of fractal structure, if properly designed substrate junctions are employed.

While substrates described above have proven useful in SERS, they generally ignore the support layer as a means to further increase signal intensity. Anderson and Moskovits address this deficiency by tethering AgNPs to an evaporated Ag film using chemical attachment.[26] In doing so the authors report efficient hotspots that can trap analyte molecules, despite steric hindrance from the molecular tethers used to hold the NPs in place. The authors first coat a Ag film with a mixture of 1,9-nonanedithiol (DT) and 1-decanethiol (MT). DT is used to link AgNPs to the Ag surface (both molecules were the analytes investigated by SERS). MT, which only binds the surface, serves as a spacer entity. By varying the ratio of DT to MT filler, the density of AgNPs on the surface can be controlled. Attachment was accomplished simply by exposing the clean Ag film first to the MT/DT solution for 30 minutes, rinsing, immersing the film in the AgNP suspension for the same amount of time, rinsing, and finally drying. The SERS response appeared to be due to hotspots generated between the tethered NP and the Ag surface, and was scalable with the concentration of DT linkers. The hotspots were said to contain approximately 30 molecules based on sample geometry and Raman measurements.

Despite impressive results in this area, the plasmonic behavior of these substrates is not actively tunable, and different substrates must be fabricated to efficiently harness different excitation sources. An interesting development in this class of SERS substrates has been made by Lee and co-workers who have generated an adaptable substrate in which the interparticle spacing can be tuned.[27] By employing Langmuir–Blodgett techniques, Lee and co-workers formed a 20 nm-AgNP physisorbed monolayer on top of a poly (*N*-isopropylacrylamide)-based thermoactive polymer which allowed for dynamic surface manipulation of the substrate. By varying the temperature of the substrate, the polymer expands or contracts, moving the adsorbed AgNPs closer or further together; spacing can be tailored from less than 5 nm to 24 nm. Since the spacing between nanoparticles can be controlled by adjusting temperature, particle spacing is actively tuned during a given SERS experiment to approach the strongest coupling between adjacent particles and to more closely match the plasmon resonance wavelength to the laser excitation wavelength. This is demonstrated by comparing the spectra of R6G at different temperatures; it appears that the signal is enhanced by one order of magnitude when the film spacing is optimized. As an interesting aside, the thermoactive polymer backing is used to ''repair'' discontinuous or broken particle films by taking a defect-containing monolayer and condensing into a closer-packed array in which more plasmonic coupling may occur, possibly allowing for a more resilient system.

Colloidal surfaces have also led to functional DNA detection systems based upon AuNP–DNA-analyte conjugates and SERS. Our group has shown AuNPs functionalized with single-stranded DNAs and Raman dyes can be captured using a three-strand system where target molecules (also single-stranded oligonucleotides) serve to bind AuNPs to an underlying chip in a microarray format.[28] These AuNPs report their position based on optical extinction, but more importantly, they facilitate the formation of a silver coating (grown from a solution of Ag^+ in reducing conditions) that acts to boost the SERS signal from the Raman dyes immobilized on the surface of these AuNPs (Fig. 4(A)). Thus, the strategy combines the high-sensitivity, high-selectivity attributes of conventional absorbance-based chip systems and the multiplexing capabilities of SERS since a very large number of probes can be designed by using a Raman tag as a spectroscopic fingerprint. In employing this system, six dissimilar DNA targets with six Raman-labeled nanoparticle probes were distinguished, as well as two RNA targets with single nucleotide polymorphisms (Fig. 4(B)). The unoptimized detection limit of this method was reported to be 20 fM (of target nucleotide concentration).

Engineered individual dimers and related systems

In the previous section, we outlined nanoparticle-modified surfaces for use as SERS substrates. From this body of work,

one can conclude that dimer structures are one important motif for the generation of the high EM fields that are responsible for a SERS hotspot. Therefore, the next logical step for generating the most efficient, effective SERS substrate is to study the synthesis of these dimers (or variants of them) directly, and gain tighter control over the characteristics that determine their SERS activity. If more regular dimers could be fabricated reproducibly, all of the properties of the SERS active structure could be investigated individually and more definitively, rather than being grouped in an ensemble where only statistical averages are feasible. This would better elucidate which parameters are particularly relevant to SERS activity. An attempt to understand the specific structures in metal colloids responsible for SERS was made by Xu and Käll who studied the photonic properties of AgNP dimers.[29] By coating 90 nm AgNP with hemoglobin (to serve as a few-nm thick spacer), the authors were able to ensure that the dimers would form with nanoscale gaps (~5 nm). The major advance of this work was to confirm, both experimentally and theoretically, that dimers are very sensitive to incident laser polarization, with the greatest SERS intensity generated when the polarization was along the axis of the dimers.

These results were expanded upon by Halas and co-workers who synthesized and studied solid nanospheres (~30 nm), hollow nanoshells (~50, 70 nm), and dimers of both these structures.[30] In these experiments, gold nanospheres and nanoshells were either purchased or prepared and dropped onto a glass substrate. In dropping a dilute suspension of particles and letting it dry, both individual particles and dimers could be isolated through careful observation of the resulting film. By studying the SERS properties and characterizing the studied structures *in situ*, Halas and co-workers were able to probe the question of Raman enhancement's relationship to dimer structure (albeit, this dimer structure was randomly generated, it allowed for rational study) (Fig. 5(A)). Using *p*-mercaptobenzoic acid (4-MBA) as a SERS analyte under 633 nm excitation, it was found that while individual Au nanoparticles did not exhibit an appreciable SERS intensity, individual nanoshells did, and the nanoshells did not exhibit SERS signal as strongly as nanosphere dimers. These experimental observations were confirmed by theoretical finite difference time domain studies (Fig. 5(B)). It should be noted that in these studies the excitation laser polarization needed to be along the interparticle axis in order to provide the maximum enhancement, confirming previous studies. The dimer structures studied, whether they are from particles or shells, all had interparticle spacing of less than 20 nm. This work, along with the work of Xu and Käll, while not completely rationally designed, suggests that dimer structures are responsible for the enhanced EM fields necessary for SERS.

After experimental and theoretical work established dimers as the likely source of SERS hotspots, groups began work on creating controlled dimer structures. Theoretical work predicting that dimers of anisotropic particles may be best for generating large EFs prompted Moerner and co-workers to fabricate substrates containing Au "bowtie" nanostructures.[11] Each "bowtie" consisted of two electron-beam lithographically (see lithography section below) generated triangles approximately 100 nm on a side, 18 nm thick, and with a sub

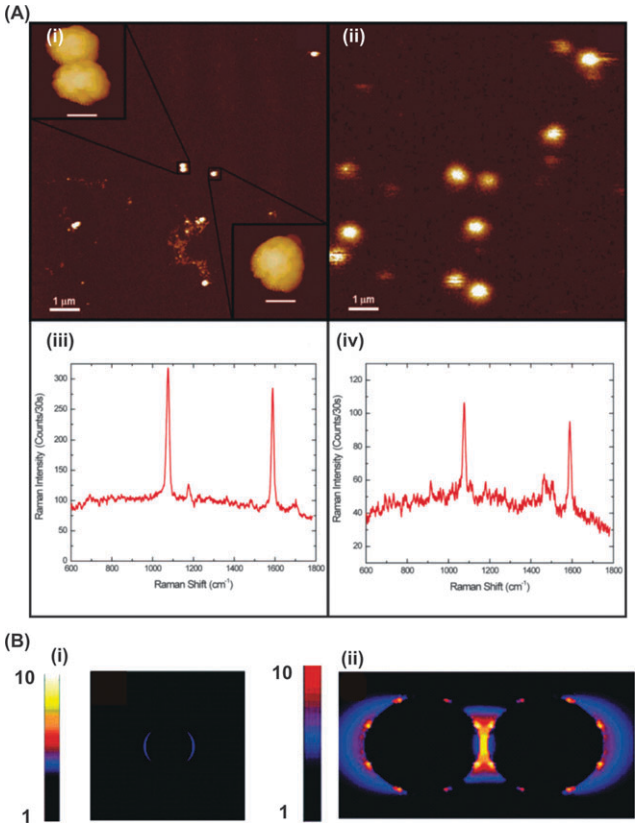

Fig. 5 Nanoparticle dimers from ref. 30. (A) Atomic force micrograph of (i) Au nanoshells. Insets show high-resolution images of two nanoshells. Scale bar in insets denote 100 nm. (ii) Confocal micrograph of inelastically scattered light from 4-MBA coated nanoshells immobilized on silane coated glass substrates. (iii) SERS spectrum of adjacent nanoshell pair from top-left insert in (i). (iv) SERS spectrum of individual nanoshell from lower right insert in (i). (B) Electromagnetic near-field enhancement at the excitation laser's wavelength (633 nm) for (i) an isolated Au nanosphere and (ii) an adjacent nanosphere pair with interparticle axis parallel to the incident polarization. (Reprinted with permission. Copyright 2005, American Chemical Society.)

20-nm junction formed at the junctions of two vertices, one from each triangle. The authors coated these dimers with *p*MA and studied the enhancement mechanism, paying special attention to identify and assign contributions to the EF from either electromagnetic or chemical sources. Since the structures had known dimensions and were stable and highly reproducible, the EM contribution to the SERS response should remain constant if the illumination and substrate structure is controlled. Accordingly, variations in chemical enhancement (CE) would be responsible for observed variations in the EF if any existed. In studying time-lapse *p*MA spectra, some modes (such at the 1077 cm^{-1} C–S stretch) were unchanged over time, while others exhibited dramatic intensity swings. It was postulated that these widely varying modes were due to a small number of molecules that experience large changes in the chemical enhancement, as much as by a factor of 10^7. Because CE is closely related to charge transfer mechanisms, the authors postulate this behavior was due to varying orientations of the adsorbates relative to the surface,

which would change how the adsorbates' molecular orbitals interact with the substrate, in turn effecting charge transfer conditions. Accordingly, Raman modes corresponding to the aromatic character of the *p*MA, where the aromatic ring can switch from standing vertically away from the surface to lying flat on the Au surface, exhibit wide variations in EF; modes not greatly affected by these orientation changes (*e.g.* C–S stretches in *p*MA) do not exhibit high variability in their Raman signature. This work is one illustration of how a rationally designed substrate could be engineered with high reproducibility to probe the fundamental mechanisms of SERS.

Similar work was attempted by Murakoshi and co-workers who constructed Ag dimer structures and studied the structures under aqueous conditions.[31] In this system, an array of dimers was fabricated using angle-resolved nanosphere lithography (see "lithographic techniques" below). By using a water immersion lens, the authors were able to study the SERS properties of coadsorbed 4,4′-bipyridine and 2,2′-bipyridine on dimer structures in an aqueous environment. The authors deposited a monolayer of microparticles on a surface, evaporated Ag employing the microparticles as a mask, and deposited Ag in the interstitial sites between close packed spheres. The substrate was tilted, a second layer of Ag evaporated, and the templating spheres removed. The resulting substrate is an array of triangular AgNP dimer structures consisting of one large and one small triangle each (the edge length of the large triangle was approximately 75 nm, the edge length of the smaller triangle was approximately 45 nm). By controlling the relative angle the substrate is tilted during the metal evaporation in the lithography step, the spacing of a gap generated between the dimer structure could be tuned until EF was maximized. In this system the authors report an EF between 10^5 to 10^9, with maximum SERS response when the laser excitation was polarized along the long axis of the dimer. Maximum signal arose when a relative deposition tilt of 17° was used. The exact gap dimensions were not given, but this seemed to correspond to a situation when the gap is nearly minimized, and any further attempts at gap narrowing led to the fabrication of one anisotropic structure (with decreased SERS activity) rather than a true dimer. Through analysis of the Raman spectra of the coadsorbed analyte, Murakoshi and co-workers deduce that a very small number of molecules are present in the dimer.

One intriguing approach for fabricating dimer structures was developed by our group. By leveraging a technique called "on-wire lithography", we were able to fabricate linear arrays of disks, separated by finely controlled gaps.[9] A 360 nm-diameter multisegmented nanowire made of alternating Au and Ni was synthesized by employing a template-directed electrochemical synthesis, which involves electrochemically reducing metal ions in cylindrical, aligned pores of aluminium oxide. A SiO_2 backing was deposited along one-half of the circumference of the rod by plasma-enhanced chemical vapor deposition. This was followed by chemical etching of the nanorods' Ni segments. Using this method, the authors were able to synthesize arrays of dimers, trimers, tetramers and pentamers with a spatial resolution as low as 2.5 nm (Fig. 6(A)). Due to the nature of the process, multiple dimers and dimer-like structures of varying geometries could be synthesized on one array, allowing for internal controls and direct comparison of relative Raman intensity of each structure with a confocal Raman microscope. Also of note is that these arrays were dispersible, allowing for colloidal functionalization techniques.

Due to the flexibility of the approach, direct comparisons between different types of dimers, trimers and tetramers of varying gap spacing and thickness could be made. This allows for testing of the nearby structure of colloidal aggregates for impact on the dimer hotspots. After functionalizing the arrays

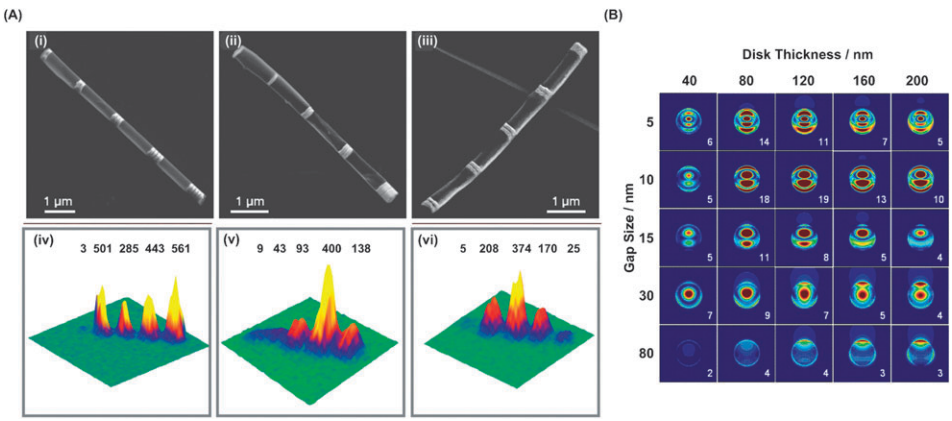

Fig. 6 OWL-Generated nanodisk arrays from ref. 9. (A) Scanning electron microscopy images of (i) monomers through pentamers of 120 ± 10-nm Au disks with 30 ± 5-nm separations. (ii) Au disk with identical 30 ± 5-nm separations and thicknesses of 40 ± 5, 80 ± 8, 120 ± 10, and 200 ± 15 nm from top left to bottom right. At the top left is a single Au disk (thickness ± 40 nm). (iii) Identical 120 ± 10 nm Au disks with separations of 160 ± 10, 80 ± 10, 30 ± 5, 15 ± 5, and 5 ± 2 nm from bottom left to top right. (iv), (v), (vi), are 3D confocal Raman images of the structures shown in (i), (ii) and (iii). Numbers indicate intensity in arbitrary units. (B) Electric field enhancement (contours of $|E|^2$) for disk dimers composed of identical Au disks with different thicknesses and gap distances. In columns 1–5, the disk thicknesses are 40, 80, 120, 160 and 200 nm, respectively. In rows 1–5, the gap distances are 5, 10, 15, 30 and 80 nm, respectively. Contours vary from 0 (blue) to 50 (red) times the incident field intensity. The number in the lower right corner of each image is $|E|^2$ relative to the isolated particle result. (Reprinted with permission. Copyright 2006, National Academy of Sciences, USA.)

with MB and excitation with a 633 nm laser, it was found that 120 nm thick dimers with 30 nm gap spacing produced the optimal response (over 100 times the intensity of a single disk) (Fig. 6(A)). These empirical results were correlated with theoretical models using the discrete-dipole approximation (DDA). For this system, the DDA approach predicted that maximum EF was generated by 120 nm thick disks separated by 10 nm provided optimal response (Fig. 6(B)). These predictions are in qualitative agreement with the experimental results in that a 120 nm thick disk pair with non-minimal (30 nm) gap spacing led to the greatest SERS response. One possibility for these small differences in the theoretical and empirical results is that the surface roughness on the disk pairs led to an effectively narrower spacing than the TEM defined 30 nm gap.

This work was recently expanded upon by our group using these linear arrays of dimers (each with the optimized geometry) to make "nanodisk codes" (NDCs).[10] In these studies, we were able to make a binary-reporting scheme capable of high-sensitivity, multimodal reporting for both chemical and physical covert labeling as well as biomolecule detection by controlling the spatial location of the disk dimers along the length of the array. With NDCs, one has the inherent ability to employ labeling chromophores and physical architecture in redundant (where the dye label reporter serves to confirm the binary encoding data), collective (where both the label and the architecture give complementary encoding information), or independent methodologies (where only the label or binary structure is used). We have used such nanostructures in biodetection schemes for oligonucleotides with an unoptimized limit of detection of 100 fM. Importantly, different NDCs can be used to simultaneously probe for multiple targets in one solution. This technique takes advantage of the narrow vibrational line signatures afforded by Raman spectroscopy (as opposed to the broad emission bands associated with fluorophores), and in principle, could facilitate the use of a much larger library of dyes for encoding and multiplexing purposes than fluorophores-based techniques.

Dimers have been studied in a variety of other settings as well. Berlin and co-workers[32] have developed composite organic–inorganic nanoparticles (COINs) by inducing aggregation of small amounts of Ag or Au colloids to form dimer-like aggregated structures which behave as Raman hotspots and Moskovits and co-workers[33] have generated Ag in dimer-like structures using silica MSs as a template, Berlin and co-workers began by forming $\sim$50–100 nm NPs in solution. During ripening, the authors added Raman labels to solution, asserting that the adsorption of the dye reduced electrostatic repulsion and led to small-scale aggregation. Finally, the COINs were functionalized with antibodies that served to both stabilize the nanostructures in solution and allow multiplexed sandwich-type immunoassays to be performed. By using the antibodies to target analyte proteins, the SERS-active COINs could be used to enhance and decode mixtures of Raman-active molecules in the COIN itself.

Moskovits and co-workers based their system on $\sim$880 nm SiO_2 microspheres. These MSs were tightly packed by ultracentrifugation and the exposed regions of the MSs were passivated with a polyethylene glycol derivative. The MSs are subsequently redispersed and the unpassivated regions (resulting from where the originally closely-packed MSs were touching) are functionalized with AgNPs. Finally, short dithiol molecules are used to cross-link these SiO_2/AgNP hybrids to form the SERS hotspots; in using the 1,4-benzenedithiol or a longer thioacetyl-terminated oligo(phenylenevinylene) molecule, the interparticle gap can be tuned. A major attribute of this system is that the location of the hotspots can be easily and reliably found using optical microscopy, eliminating the need to tediously hunt for regions of high SERS signals by less convenient means. The authors report that (using the linker molecules as reporters) these hotspots exhibit the same Raman spectra as those collected using colloidal dispersions as a substrate, but can be obtained with much less integration time. They estimate the EF of the hybrid particle junctions to be $\sim 10^8$ to 10^9 (however the crosslinkers used to measure SERS response may be resonant). This is an intriguing system in that it allows quick spatial location and Raman readout, however, the system has not been demonstrated with a non-cross linking, nonfunctional analyte.

Anisotropic non-nanosphere-based engineered substrates

SERS is expected from anisotropic materials, because symmetry breaking allows for more complex plasmon propagation, potentially leading to more intense EM field generation along the structure and in gaps formed between these materials. The most obvious example of this phenomenon can be found in nanorods, which contain a long axis that induces multipolar plasmon activity. Tian and co-workers and Moskovits and co-workers have both fabricated nanorods employing template-directed synthesis techniques.[34,35] Tian and co-workers compared Cu, Ag, Au, Ni, and Co nanowires of different widths and lengths (even though Ni and Co are typically considered SERS-inactive, a slight response was observed) while Moskovits and co-workers focused on Ag nanowires. Using benzenenitrile as their analyte, Tian and co-workers found that nanowire substrates exhibited greater SERS activity than that of a randomly roughened surface, and that the orientation of the NWs was critical. As the membrane supporting the nanowires is dissolved, SERS intensity is shown to increase. The authors state that this is related to the changing plasmonic properties of the array as the supporting matrix is removed. However, if too much of the supporting alumina membrane was dissolved, the nanowires rearranged from a vertical, parallel orientation to randomly lying flat on the surface of the substrate. When this transition occurred, SERS activity decreased, implying the vertical, ordered relationship was important to SERS response.

Moskovits and co-workers observe very similar results. Because the AgNWs are protected by the alumina matrix when they are grown, selective functionalization of the nanorods (*i.e.* only placing analyte on the tips of the nanowires) is possible. In this case, the nanowires are exposed to an analyte solution while still in the alumina membrane leaving only the ends of the AgNWs exposed and consequently functionalized. The membrane can subsequently be (fully or partially) removed. Upon removal of the templating matrix, the nanowires

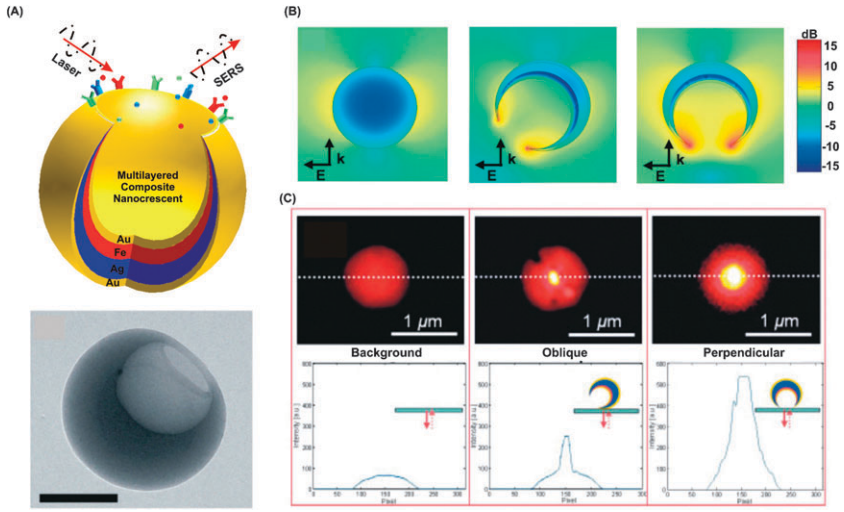

Fig. 7 Composite magnetic nanocrescents from ref. 36. (A) (top) Schematic diagram of SERS detection on a single composite nanocrescent (bottom) transmission electron microscopy image of a single magnetic nanocrescent SERS probe. The scale bar represents 100 nm. (B) Simulated local electric-field-amplitude enhancement in dB by a single nanocrescent oriented 0° (right) and 45° (middle) with respect to the 785 nm light incident direction, in comparison with an 80 nm Au nanosphere (left). (C) Intensity images and the cross-line intensity plots of a laser focal spot without a nanocrescent (left), and with a single nanocrescent obliquely (middle) and perpendicularly (right) oriented with respect to the direction of excitation laser light. (Reprinted with permission. Copyright 2005, Wiley-VCH Verlag GmbH & Co. KGaA.)

bundle together to generate SERS hotspots. Because it is possible to localize analytes near where the AgNWs meet (the tips), it is also possible to maximize Raman intensity per analyte molecule. The authors report that adding the analyte, and then etching the template produces better EFs than etching prior to functionalization. Furthermore, there is an optimal etch time for each of the templates where supporting template is partially removed, allowing the nanowires to aggregate, but not so much that gaps generated between the AgNWs close up and inhibit local EM activity.

In addition to metal nanowires, more complex structures have been fabricated. Lee and co-workers have developed three-dimensional crescent-shaped nanoparticles that contain a sub-10 nm gap that eliminates the need for multiple particles to form a dimer or other plasmonic superstructure in order to generate large EFs.[36] In the latest iteration of the technology, these nanocrescents contain a sandwich structure consisting of Au, Fe, Ag and Au (Fig. 7(A)). To fabricate these structures, the authors drop-cast 150 nm polystyrene colloids onto photoresist and let the suspension settle and dry. Metals were evaporated in series onto the surface at a 60° tilt angle while rotating at 60 rpm. The optimal type and relative amount of metal was determined with the aid of finite element analysis (Fig. 7(B)). Lift-off and dissolution of the polystyrene spheres leads to a suspension of nanocrescents.

One interesting property of these structures is that they generate local field enhancement in the NIR due to the dual tip-nanoring geometry in the active region. This NIR activity makes the crescent structures interesting for biodetection applications since NIR light interferes less with living tissues compared to visible or UV radiation. To aid in this application, Lee and co-workers employ an Fe layer on the interior of the crescent to make the object magnetically active (Fig. 7(C)). This layer allows the crescent to be moved and rotated by a magnetic field. As with most anisotropic structures, Raman enhancement was quite sensitive to excitation polarization, and (using 3-mercaptopropyltrimethoxysilane) an EF of 10^6 for a single crescent was reported. The authors argue that the EF could be as large at 10^8 if the relative amount of analyte to solvent in the hotspot is taken into account.

Electromigrated or mechanical junctions

To make junctions that could be studied on an individual basis with very high control over the geometry of the gap, researchers have used electromigration or mechanical break junctions when throughput is not an issue. Most of these techniques yield dimer-like structures with precisely size-controlled gaps similar to those discussed above and can be often used to simulate free-standing dimer structures. In this regard Tian and co-workers, have studied gaps as small as ~1 nm (the end gap length was estimated by tunneling measurements).[37] By using a piezoelectric component, the authors are able to electromechanically adjust the junction spacing. After the gap was functionalized with 1,4-benzenedithiol and *p*MA, the system was characterized by SERS under 633 nm excitation. Unsurprisingly, the gap region exhibited stronger SERS response than the smooth sections of the electrode or their edges. By using the piezo to manipulate the gap size, it was found that a separation of 4 Å produced optimal SERS enhancement, but the authors caution that the procedure is not highly reproducible as of yet, with only 20% of the substrates demonstrating a distance-dependent response. In all cases, and consistent with previous results (*vide supra*), much stronger enhancement was generated when the laser was polarized along the axis of the microelectrodes forming the junction.

Natelson and co-workers have employed electromigration techniques to fabricate rationally designed, SERS-based structures, where they believe sensitivity approaches single-

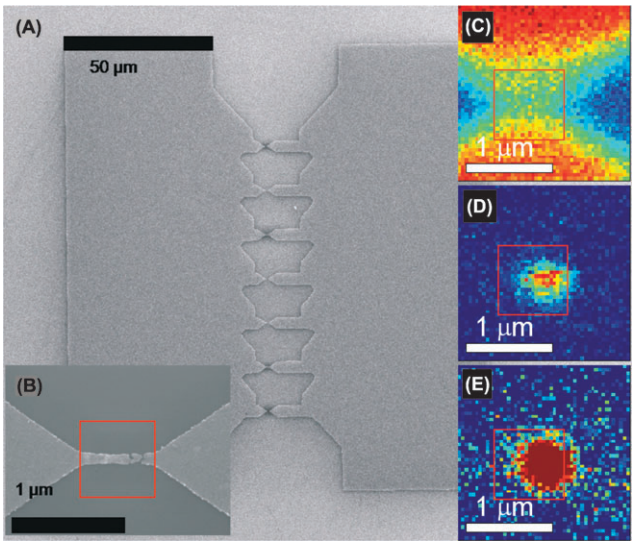

Fig. 8 Electromigrated gaps from ref. 38. (A) Full multibowtie structure, with seven nanoconstrictions. (B) Close-up of an individual constriction after electromigration. Note that the resulting nanoscale gap ($\leq$5 nm at closest separation, as inferred from closer images) is toward the right edge of the indicated red square. (C) Map of Si Raman peak (integrated from 500 to 550 cm^{-1}) in device from (B), with red corresponding to high total counts. The attenuation of the Si Raman line by the Au electrodes is clear. (D) Map of *p*MA SERS signal for this device based on one carbon ring mode (integrated from 1050 to 1110 cm^{-1}). (E) Map of integrated low-energy background (50–300 cm^{-1}) for this device. (Reprinted with permission. Copyright 2007, American Chemical Society.)

molecule detection levels.[38] The authors start by using electron-beam lithography to pattern a series of "bowtie" structures that consist of two larger ($\sim$50 μm $\times$ 150 μm) pads connected by thin, tapered bridges measuring 80–100 nm wide. By passing current though these thin junctions, momentum from current-carrying electrons is transferred to the Au lattice, rearranging atomic positions, eventually leading to a break in the thin Au section (Fig. 8(A), (B)). This process can be done by manually or automatically monitoring the resistance of the junction, and the authors found that a post-migration resistance of $\sim$10 kΩ was optimal for their experiments, and resulted in a gap of approximately 5 nm or less. This procedure has limited reproducibility, with 43% of the substrates having a final resistance less than 25 kΩ. Subsequently, the gaps are functionalized with *p*MA or other small molecules, and a confocal microscope with 565 nm excitation is used to study the gaps (Fig. 8(C)–(E)). Interestingly, blinking of intensity and spectral diffusion, hallmarks of few- or single-molecule systems, is routinely observed. After a estimation of the hotspot geometry (effective radius 2.5 nm), the authors speculate the EF for this device is 5×10^8, theoretically allowing for 100 molecule-detection at a single hotspot.

Lithography techniques

Given that SERS intimately depends on the nanostructure of the substrate, perhaps the most obvious techniques to pattern substrates and generate large SERS activity would be lithographically based. However, most lithographic techniques are not capable of producing feature sizes small enough to be truly SERS-active. The most obvious exception is electron-beam lithography (EBL), which has been routinely used to fabricate structures as small as 15 nm, and can produce smaller structures ($\sim$5 nm) in exceptional cases. In EBL, a substrate is first coated with a material called a photoresist that will respond to a concentrated electron beam (usually partially disintegrating, but some resists can harden and produce "negative" features). Then, an electron beam is used to generate patterns within the photoresist material. The substrate/photoresist is rinsed with a solvent that will remove the photoresist damaged by the electron beam, but not photoresist that was unharmed. What results is a patterned surface, which can serve as a mask for metal evaporation. Upon evaporation of the metal and subsequent removal of all photoresist by a solvent in which it is completely soluble, metal nanostructures matching the electron beam pattern remains on the substrate. As noted above, Moerner and colleagues employed EBL to make "bowtie" dimer structures,[11] however in fabricating a grating of Au disks, Lévi and co-workers earlier demonstrated EBL could be a feasible method to generate SERS structures. This work culminated with the report of an optimized Au grating consisting of elongated Au particles with major and medium axes of 154 and 120 nm, respectively.[12] These particles are 40 nm high and separated by 500 nm in both *x* and *y* directions. Through a combination of theoretical and empirical studies, it was found that the maximum SPR of the AuNPs is at the midpoint between the wavelength of the exciting laser and the Raman line. The structures were designed to take advantage of this relation. In using BPE as an analyte across different laser excitations (633, 647, 676 nm) and polarizations (parallel to long axis, perpendicular to long axis), the authors concluded the optimized structure was able to produce an EF 10^5 to 10^6.

While EBL is one of the few conventional lithographic processes able to effectively and routinely pattern substrates on length scales meaningful for SERS, new techniques also have been invented and applied to this problem. An example of such non-conventional methods is nanoimprint lithography (NIL). NIL creates patterns by mechanical deformation of imprint resist. First, a mold is made by conventional lithography such as EBL or photolithography and is typically fabricated out of a hard material. The imprint resist is generally a monomer or polymer formulation that has been cured by heat or UV light during the imprinting. Post processing is similar to other lithographic techniques, with developing, and metal evaporation used to from the final structure. Fenniri and colleagues employ this technique to form a variety of different Ag substrates for SERS. The authors controlled particle shape and size, and subsequently compared their SERS properties.[13] Multiple structures were generated: $\sim$30–60 nm AgNPs deposited on smooth surfaces (the control), these same AgNPs in groupings on 150 nm thick, 120 nm high lines separated by 50 nm, and these AgNPs grouped on three sizes of pillars: 125 nm $\times$ 125 nm $\times$ 120 nm, 100 nm $\times$ 80 nm $\times$ 120 nm, and 60 nm $\times$ 40 nm $\times$ 120 nm pillars, all with a periodicity of 200 nm. The structures were functionalized with 2-naphthalenethiol and their SERS response was probed with both 532 nm and 780 nm laser excitations. As expected,

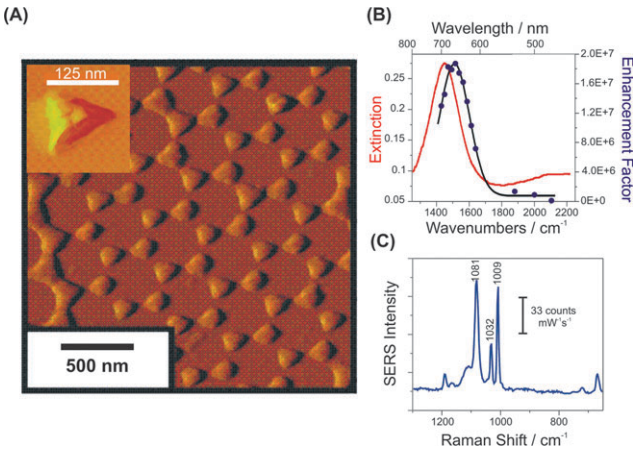

Fig. 9 Nanosphere lithography-generated structures from ref. 7. (A) Tapping-mode AFM image of a representative array surface. Inset: a close up of one triangle. (B) LSPR spectrum (solid line, λ_{max} = 688 nm, FWHM = 95 nm) and WS-SERES spectra (data points) for the 1081 cm^{-1} band of benzenethiol measured from a Ag nanoparticle array surface. (C) SERS spectrum of benzenethiol measured from Ag nanoparticle array surface (λ_{ex} = 532 nm, power = 3.0 mW, 100 s data acquisition time). (Reprinted with permission. Copyright 2005, American Chemical Society.)

substrate structure greatly impacted SERS activity. With 532 nm excitation, the AgNPs immobilized on the parallel line structure showed the greatest enhancement of all structures relative to the plain AgNP standard film. Under 780 nm excitation, the 100 nm × 80 nm × 120 nm pillar sample showed the greatest response. The authors conclude that NIL is a useful method to rationally control surface topology, which in turn will cause differences in plasmon coupling that can be tuned to optimize SERS response for a given excitation.

No discussion of lithographically generated structures for SERS would be complete without a discussion of nanosphere lithography. NSL is similar to the colloidal crystal techniques discussed above in that it uses micro- or nanospheres to template metal evaporation, leading to plasmonically active nanostructures. By coating substrates with these nanospheres, drying them in a close-packed arrangement and evaporating metal onto the substrate, ''metal over nanoparticle'' structures (*vide supra*) can be fabricated. These structures can then be used to perform SERS experiments. However, if the templating spheres are removed, arrays of silver triangles result from where the evaporated metal penetrated the interstitial locations result (Fig. 9(A)).[7] The simplicity of this process is its strength: both the metal film over nanoparticle and NSL triangle arrays are interesting since the local surface plasmon resonance (LSPR) and SERS activity can be easily studied and closely correlated.

In addition to the metal-over nanosphere approach described above,[5,6] SERS has been observed for NSL-generated surfaces and used to glean information about fundamental SERS phenomena. One example of this is found in the work of Van Duyne and co-workers which uses these triangle arrays to study wavelength-scanned surface-enhanced Raman excitation spectroscopy (SERES), a technique where SERS enhancement is measured over a variety of laser excitation wavelengths (Fig. 9(B)).[8] In using this Ag nanotriangle array (generated by performing NSL with ~450 nm nanospheres, producing triangles with ~200 nm long edges), the authors were able to correlate LSPR and the SERES profile in a much more tightly controlled manner than most researchers had in the past. Because the LSPR is the effective ''antenna'' that amplifies light in SERS hotspots, understanding its character could help to understand and more effectively harness the SERS phenomena. In this case, the authors were able to determine that each substrate shows a SERES profile that has a similar line shape to the extinction spectrum of the substrate, and that the largest relative SERS intensity occurs when the LSPR maximum is located between the excitation and vibration wavelengths. Under these conditions, both the incident and scattering photons experience enhancement by the LSPR, directly demonstrating that the strongest SERS enhancement occurs when both the incident and Raman scattering photons are both strongly enhanced. Employing the NSL-generated substrate, EFs of approximately 10^8 were achieved (benzenethiol was used as the analyte). Of course, conventional SERS spectra can be gleaned through use of this substrate as well (Fig. 9(C)).

Conclusions

A decade ago, the major criticisms of SERS concerned irreproducibility in signal and a weak understanding of the types of structures that would yield large and reproducible enhancements. Since then, major strides have been made in understanding the phenomenon, and with the advent of nanotechnology, new strategies have been developed to make either dispersible micro- or nanoscopic structures or macroscopic nanopatterned substrates that yield larger and more reproducible responses. In the work described in this review, this trend is apparent. While the range of enhancement factors observed (in terms of absolute magnitude) has not markedly changed since the first high-enhancing SERS experiments were reported (EFs ranging from 10^6 to 10^9 or higher), the larger number of independent groups now reporting these results, as well as the reproducibility of these measurements serve as an indication of recent trends.[31,33]

In addition, powerful proof-of concept applications pertaining to small-molecule and biodetection, have all been evaluated. These nanostructures have allowed fundamental study of the SERS phenomenon and elucidated new details about the nature of the effect. Among these advances are a greater understanding of the chemical enhancement mechanisms, empirical verification of theoretically-predicted optimal plasmonic structures, and answers to questions pertaining to the optimum coupling between excitation sources and the substrate. However, these fundamental advances are only half the story; new, engineered substrates have also allowed applications-driven work to flourish. Progress in SERS research has attracted the attention of scientists from multiple disciplines, and these researchers have begun to develop new substrates of their own or apply existing substrates to new applications. For example, work on biosensors has been prominent with the development of nucleic acid,[28] pathogen,[6] immuno- (including cancer markers),[39–41] and glucose[42] assays.

Work on fundamental studies in SERS continues to drive interest in the field. This cycle of understanding, innovation, and application continues to progress, promising more advances in SERS research and technology to follow. Although these applications and substrates are promising advances, we still need a much greater understanding of how to control surface architecture in order to stabilize and maximize the SERS response. Even in the work described in this review, imperfections in substrates and their nanostructures have a significant effect on the ultimate SERS response observed. Applications of SERS either must be made more tolerant of these inconsistencies or ways of exerting better control of surface nanoarchitecture must be developed. However, with so much interest in the field and the rapid developments in nanotechnology, the future of SERS remains promising.

Acknowledgements

J.E.M. acknowledges the Northwestern University Presidential Fellowship; C.A.M. acknowledges the NSF-NSEC, AFSOR, and NCI-CCNE for support of this work.

References

1 G. A. Ozin and A. C. Arsenault, *Nanochemistry: A Chemical Approach to Nanomaterials*, The Royal Society of Chemistry, Cambridge, UK, 2005.
2 A. Campion and P. Kambhampati, *Chem. Soc. Rev.*, 1998, **27**, 241–250.
3 M. Moskovits, *J. Raman Spectrosc.*, 2005, **36**, 485–496.
4 G. A. Baker and D. S. Moore, *Anal. Bioanal. Chem.*, 2005, **382**, 1751–1770.
5 L. A. Dick, A. D. McFarland, C. L. Haynes and R. P. Van Duyne, *J. Phys. Chem. B*, 2002, **106**, 853–860.
6 X. Zhang, J. Zhao, A. V. Whitney, J. W. Elam and R. P. Van Duyne, *J. Am. Chem. Soc.*, 2006, **128**, 10304–10309.
7 A. J. Haes, C. L. Haynes, A. D. McFarland, G. C. Schatz, R. P. Van Duyne and S. Zou, *MRS Bull.*, 2005, **30**, 368–375.
8 A. D. McFarland, M. A. Young, J. A. Dieringer and R. P. Van Duyne, *J. Phys. Chem. B*, 2005, **109**, 11279–11285.
9 L. Qin, S. Zou, C. Xue, A. Atkinson, G. C. Schatz and C. A. Mirkin, *Proc. Natl. Acad. Sci. U. S. A.*, 2006, **103**, 13300–13303.
10 L. Qin, M. J. Banholzer, J. E. Millstone and C. A. Mirkin, *Nano Lett.*, 2007, **7**, 3839–3853.
11 D. P. Fromm, A. Sundaramurthy, A. Kinkhabwala, P. J. Schuck, F. S. Kino and W. E. Moerner, *J. Chem. Phys.*, 2006, **124**, 061101.
12 N. Félidj, J. Aubard, G. Lévi, J. R. Krenn, A. Hohenau, G. Schider, A. Leitner and F. R. Aussenegg, *Appl. Phys. Lett.*, 2003, **82**, 3095–3097.
13 R. Alvarez-Puebla, B. Cui, J.-P. Bravo-Vasquez, T. Veres and H. Fenniri, *J. Phys. Chem. C*, 2007, **111**, 6720–6723.
14 E. C. Le Ru, E. Blackie, M. Meyer and P. G. Etchegoin, *J. Phys. Chem. C*, 2007, **111**, 13794–13803.
15 B. Pettinger, *Top. Appl. Phys.*, 2006, **103**, 217–240.
16 P. Verma, Y. Inouye and S. Kawata, *Top. Appl. Phys.*, 2006, **103**, 241–260.
17 A. Hartschuh, H. Qian, J. Meixner, N. Anderson and L. Novotny, *Surf. Interface Anal.*, 2006, **38**, 1472–1480.
18 A. F. McCabe, C. Eliasson, R. A. Prasath, A. Hernandex-Santana, L. Stevenson, I. Apple, P. A. G. Cormack, D. Graham, W. E. Smith, P. Corish, S. J. Lipscomb, E. R. Holland and P. D. Prince, *Faraday Discuss.*, 2006, **132**, 303–308.
19 R. G. Freeman, K. C. Grabar, K. J. Allison, R. M. Bright, J. A. Davis, A. P. Guthrie, M. B. Hommer, M. A. Jackson, P. C. Smith, D. G. Walter and M. J. Natan, *Science*, 1995, **267**, 1629–1632.
20 D. J. Maxwell, S. R. Emory and S. Nie, *Chem. Mater.*, 2001, **13**, 1082–1088.
21 H. Wang, C. S. Levin and N. J. Halas, *J. Am. Chem. Soc.*, 2005, **127**, 14992–14993.
22 D. M. Kuncicky, B. G. Prevo and O. D. Velev, *J. Mater. Chem.*, 2006, **16**, 1207–1211.
23 S. Kubo, Z.-Z. Gu, D. A. Tryk, Y. Ohko, O. Sato and A. Fujishima, *Langmuir*, 2002, **18**, 5043–5046.
24 M. Baia, L. Baia and S. Astilean, *Chem. Phys. Lett.*, 2005, **404**, 308.
25 Z. Wang, S. Pan, T. D. Krauss, H. Du and L. J. Rothberg, *Proc. Natl. Acad. Sci. U. S. A.*, 2003, **100**, 8638–8643.
26 D. J. Anderson and M. Moskovits, *J. Phys. Chem. B*, 2006, **110**, 13722–13727.
27 Y. Lu, G. L. Liu and L. P. Lee, *Nano Lett.*, 2005, **5**, 5–9.
28 Y. C. Cao, R. Jin and C. A. Mirkin, *Science*, 2002, **297**, 1536–1540.
29 H. Xu and M. Kall, *ChemPhysChem*, 2003, **4**, 1001–1005.
30 C. E. Talley, J. B. Jackson, C. Oubre, N. K. Grady, C. W. Hollars, S. M. Lane, T. R. Huser, P. Nordlander and N. J. Halas, *Nano Lett.*, 2005, **5**, 1569–1574.
31 Y. Sawai, B. Takimoto, H. Nabika, K. Ajito and K. Murakoshi, *J. Am. Chem. Soc.*, 2007, **129**, 1658–1662.
32 X. Su, J. Zhang, L. Sun, T.-W. Koo, S. Chan, N. Sundararajan, M. Yamakawa and A. Berlin, *Nano Lett.*, 2005, **5**, 49–54.
33 G. Braun, I. Pavel, A. R. Morrill, D. S. Seferos, G. C. Bazan, N. O. Reich and M. Moskovits, *J. Am. Chem. Soc.*, 2007, **129**, 7760–7761.
34 J. L. Yao, G. P. Pan, K. H. Xue, D. Y. Wu, B. Ren, D. M. Sun, J. Tang, X. Xu and Z. Q. Tian, *Pure Appl. Chem.*, 2000, **72**, 221–228.
35 S. J. Lee, A. R. Morrill and M. Moskovits, *J. Am. Chem. Soc.*, 2006, **128**, 2200–2201.
36 G. L. Liu, Y. Lu, J. Kim, J. C. Doll and L. P. Lee, *Adv. Mater.*, 2005, **17**, 2683–2688.
37 J.-H. Tian, B. Liu, X. Li, Z.-L. Yang, B. Ren, S.-T. Wu, N. Tao and Z.-Q. Tian, *J. Am. Chem. Soc.*, 2006, **128**, 14748–14749.
38 D. R. Ward, N. K. Grady, C. S. Levin, N. J. Halas, Y. Wu, P. Nordlander and D. Natelson, *Nano Lett.*, 2007, **7**, 1396–1400.
39 J. Ni, R. J. Lipert, G. B. Dawson and M. D. Porter, *Anal. Chem.*, 1999, **71**, 4903–4908.
40 R. G. Freeman, W. E. Doering, I. D. Walton, S. G. Penn, G. Davis, F. Wong and M. J. Natan, *Proc. SPIE–Int. Soc. Opt. Eng.*, 2005, **5705**, 114–122.
41 D. O. Ansari, D. A. Stuart and S. Nie, *Proc. SPIE–Int. Soc. Opt. Eng.*, 2005, **5699**, 82–90.
42 D.A. Stuart, J. M. Yuen, N. Shah, O. Lyandres, C. R. Yonzon, M. R. Glucksberg, J. T. Walsh and R. P. Van Duyne, *Anal. Chem.*, 2006, **78**, 7211–7215.